# Thermal-Equilibrium Defect Processes in Hydrogenated Amorphous Silicon

Z E. Smith, S. Aljishi, D. Slobodin, V. Chu, and S. Wagner
*Department of Electrical Engineering, Princeton University, Princeton, New Jersey 08544*

P. M. Lenahan
*Department of Engineering Science and Mechanics, The Pennsylvania State University, University Park, Pennsylvania 16802*

and

R. R. Arya and M. S. Bennett
*Solarex Thin Films Division, Newtown, Pennsylvania 18940*
(Received 12 March 1986; revised manuscript received 15 September 1986)

The first experimental evidence for a thermal-equilibrium defect density in undoped hydrogenated amorphous silicon, a metastable material, is presented. The defect density is in thermal equilibrium at temperatures above 200 °C; the defects measured at room temperature are largely those frozen in during cooling from the equilibrium regime. Rapid quenching reversibly increases defect density. The defect density can be reversibly decreased by shunting of the defect-generation process during cooling. This latter technique has important implications for *a*-Si:H–based solar cells.

PACS numbers: 71.55.Jv, 71.20.+c, 81.40.Rs

In true equilibrium, silicon below the melting temperature (1415 °C) is in its crystalline form. Hydrogenated amorphous silicon (*a*-Si:H), commonly prepared from plasma or thermal decomposition of silane at 250 to 325 °C, is thought to be structurally far from equilibrium; yet many metastable effects are observed, which imply that the material is in some sort of local minimum of energy to which it can return after perturbation. The most intensely studied of these metastable effects in *a*-Si:H has been the light-induced change in optical and electronic properties known as the Staebler-Wronski effect.[1] As a clearer picture of the mechanism behind light-induced defect generation has begun to emerge,[2] attention is now turning to the nature of the initial (or "as-deposited") defects.

Working from the model of Stutzmann, Jackson, and Tsai[3] for recombination-induced silicon dangling-bond generation, it was postulated that recombination of thermally generated carriers at the commonly employed growth temperatures could result in *dark* generation of dangling-bond defects, and that most of these defects, although metastable, would be frozen in during cooling after growth.[4] The slow annealing of frozen-in defects has recently been observed in phosphorus-doped *a*-Si:H.[5] This work builds on the early observations[6] of quenched-in conductivity in P-doped *a*-Si:H; both studies, however, leave open the possibility that the effects are due to the presence of dopants. In this Letter, we present the first evidence for a temperature-dependent thermal equilibrium defect density in *intrinsic* *a*-Si:H. We identify the kinetics of the creation and removal of these defects. This work also suggests that a completely new interpretation of field-induced effects in *a*-Si:H[7,8] may be in order.

The intrinsic *a*-Si:H films used in this study were prepared in a dc glow-discharge deposition system described elsewhere[9] from undiluted silane; parallel experiments conducted on *a*-Si:H,F films grown from $SiF_4+H_2$ yielded essentially identical results. The deposition system has never been exposed to dopant gases. Characterization of optical and electronic properties included subband-gap absorption as determined by the constant-photocurrent method (CPM),[10] carrier diffusion length by the differential surface photovoltage method,[11] carrier drift mobilities, and trapping times by the transient

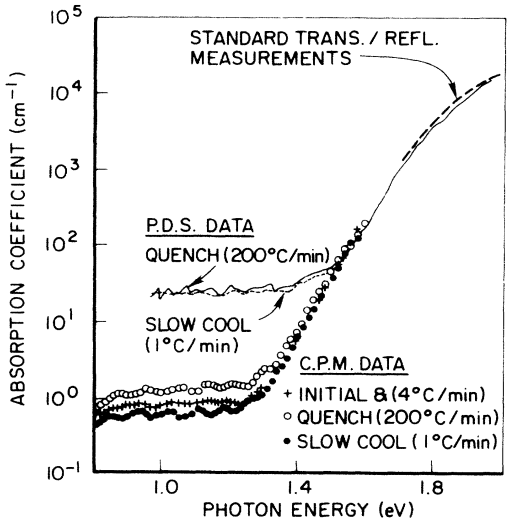


FIG. 1. Subband-gap absorption vs photon energy for a typical *a*-Si:H film in the initial state and after cooling at various rates from 300 °C. The CPM curves for the initial state and the 4 °C/min cooling state overlap within error and are drawn with one symbol (plusses).

TABLE I. Integrated subband-gap absorption (from CPM) $\int \alpha dE$, total dangling-bond density (calculated from theory) $N_{\text{total}}^{\text{calc}}$, photoconductivity $\sigma_{\text{ph}}$ (measured with 600-nm photons at a flux of $2\times10^{17}$ cm$^{-2}$ s$^{-1}$), and neutral dangling-bond density (total spins/sample volume) $N_{\text{spin}}$ for $a$-Si:H film in initial (4 °C/min cool from growth), after rapid (200 °C/min), and slow (4 °C/min) cooling from (300 °C) equilibrium.

| | $\int \alpha dE$ | $N_{\text{total}}^{\text{calc}}$ | $\sigma_{\text{ph}}$ | $N_{\text{spin}}$ |
|---|---|---|---|---|
| Initial state | $\equiv 1$ | $\equiv 1$ | $\equiv 1$ | $\equiv 1$ |
| Quenched | 1.90 | 1.8 | 0.78 | 1.27 |
| Cooled 4 °C/min | 1.00 | $\equiv 1$ | 0.98 | · · · |
| Cooled 1 °C/min | 0.64 | 0.71 | · · · | · · · |
| Uncertainty | ±5% | · · · | ±5% | ±15% |
| Normalization | 0.45 | $7.8\times10^{15}$ | $1.04\times10^{-4}$ | $5.7\times10^{15}$ |
| (units) | cm$^{-1}$ eV | cm$^{-3}$ | $\Omega^{-1}$ cm$^{-1}$ | cm$^{-3}$ |

photoconductivity time-of-flight technique,[12] neutral dangling-bond densities as determined from electron-spin resonance (ESR), and temperature-dependent dark conductivity in vacuum. Typical films exhibited spin densities of $(3-8)\times10^{15}$ cm$^{-3}$, diffusion lengths 0.1–0.3 $\mu$m, electron mobilities of $\cong 1$ cm$^2$ V$^{-1}$ s$^{-1}$, hole mobilities $\cong 5\times10^{-3}$ cm$^2$ V$^{-1}$ s$^{-1}$, and dark conductivity activation energies of 0.75–0.85 eV. These results indicate that the materials studied are comparable to the highest quality films reported in the literature.

In the first set of experiments, the subband-gap absorption spectra and photoconductivity of 2.0-$\mu$m-thick films of intrinsic $a$-Si:H (cooled from growth at a rate of 4 °C/min) were measured immediately after a 160 °C anneal (to eliminate any possible light-induced defects). The samples were then heated to 270–300 °C (the substrate temperature during film growth) in $N_2$, held there for 30 min, and then rapidly (>200 °C/min) cooled. After being measured again, the samples were heated to either 160 °C or ~300 °C and then cooled slowly (either 4 °C/min or 1 °C/min). Typical results are shown in Fig. 1. The subband-gap absorption increases dramatically with quenching, indicating the introduction of new defect states.[13,14] As shown in Table I, the integrated subband-gap absorption increases by a factor of 2 upon quenching, and this increase is removed by slow cooling.

In addition to an increase in low-photon-energy absorption, the results in Fig. 1 show an increase in the width of the absorption tail upon quenching. This increase could correspond to an increase in the valence-band-tail width of a few millielectronvolts, consistent with the idea that the band-tail widths are proportional to the temperature of freezein.[15]

Subband-gap absorption spectra were also measured by photothermal deflection spectroscopy (PDS).[13] Through a comparison of PDS and CPM spectra on a series of films covering a range of thicknesses, we have determined[16] that PDS sees transitions involving surface and near-surface states which CPM does not. Thus when the absorbances measured by these techniques are converted into effective bulk absorption coefficients, PDS curves greatly exceed CPM curves for thin films. In thick films we observe sizable changes in the PDS spectra upon quenching. The surface states appear to be unaffected by quenching. For the sample shown in Fig. 1 and Table I, the *difference* between quenched and 1 °C/min states in integrated subgap absorption $\int \Delta\alpha dE$ is 1.5 cm$^{-1}$ eV by PDS and 0.6 cm$^{-1}$ eV by CPM. By use of the appropriate prefactors[17] to convert $\int \alpha dE$ to the associated defect density, both methods find a difference in defect density of $1.1\times10^{16}$ cm$^{-3}$ between quenched and 1 °C/min states.

In Fig. 2 we show calculations of the temperature-dependent dangling-bond density theory preliminarily developed in Ref. 4. The annealing term of that theory has been modified. When the dangling-bond density is calculated for states with a distribution of activation energies, the annealing term in the time differential equation must not be integrated over energies; rather, each energy "bin" of the distribution must be time-integrated separately and the result summed. Thus the time rate of change of dangling-bond density with annealing energy $E$, $N_s^E$, is given by

$$dN_s^E/dt = c_{SW} r_t n_i^2(T) f(E) - \nu e^{-E/kT} N_s^E,$$

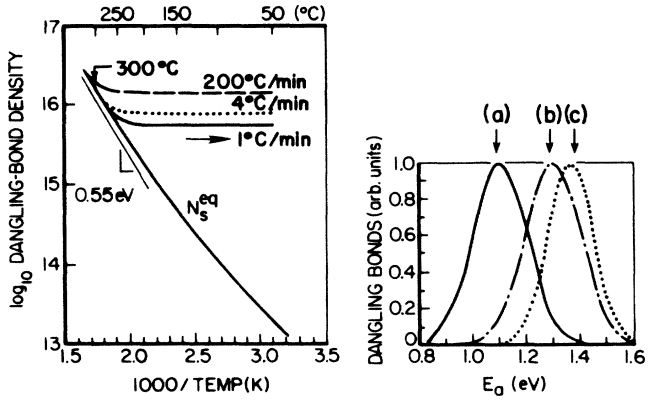


FIG. 2. Left: Calculation of temperature-dependent dangling-bond density. Right: Curve $a$, relative distribution of annealing energies of dangling bonds as created; curve $b$, the net distribution present in equilibrium at 300 °C; and curve $c$, those remaining after (4 °C/min) slow cool.

where

$$f(E)=C_1\exp\{-[(E-E_{A0})/E_W]^2/2\},$$

and

$$n_i^2(T)=[T/(300\text{ K})]^3 n_i^2(300\text{ K})e^{-E_g/kT}.$$

To compute Fig. 2 we have used the band gap $E_g=1.7$ eV, the room-temperature intrinsic carrier concentration of $n_i(300\text{ K})=1\times10^8$ cm$^{-3}$,[4] and an analytic fit to the data of Ref. 3: $c_{SW}r_t=1.5\times10^{-15}$ cm$^3$ s$^{-1}$; $\nu=1\times10^{10}$ s$^{-1}$; $E_{A0}=1.1$ eV; $E_W=0.1$ eV. These values agree with those determined from solar cell degradation and annealing characteristics.[18] $C_1$ is a normalization factor chosen such that $f(E)$ integrates to unity for a given integration step size $\Delta E$. Note that variations in parameters for which there is the greatest uncertainty or sample-to-sample variability, $c_{SW}r_t$ and $n_i^2(300\text{ K})$, have the effect of scaling the magnitude of the calculated defect density, but not changing the ratio of defects present at room temperature in the quenched versus slow-cooled states. The calculated value of frozen-in defects $N_{\text{Total}}^{\text{calc}}$ is listed in Table I.

We note in passing that recent ESR data[19] on *a*-Si:H films grown over a wide range of substrate temperatures and rapidly cooled to room temperature show an exponentially activated dangling-bond density with characteristic energy 0.57 eV. As shown in Fig. 2, our calculations predict $N_s^{eq}$ to be thermally activated with a characteristic energy of $\cong 0.55$ eV.

One of the consequences of the distribution of activation energies for annealing dangling bonds is that, when states are introduced at high temperatures, the shallow energy states anneal out and the remaining distribution is shifted to larger and larger energies. Our calculations suggest that the frozen-in states have a mean annealing energy of 1.4 eV. Annealing samples in the quenched state at 160 °C for 30 min (the standard anneal to remove light-induced defects) did not measurably alter the subband-gap absorption, while a subsequent anneal from 280 °C removed the quenched states completely.

How similar are the properties of the intrinsic defects to light-generated ones? ESR experiments were performed to see if the states frozen in are neutral dangling bonds $D^0$. The relative changes in the total number of dangling bonds (expressed as an effective bulk density in Table I) fall somewhere between the bulk (CPM) and bulk plus surface (PDS) subband-gap-absorption measurements, as one would expect if both bulk and surface dangling bonds (with various occupation probabilities) are present.[3]

Thus far we have used quenching experiments as a means of taking a snapshot of the defect density at various temperatures, observing reversible defect enhancement at temperatures above 200 °C. The parameter tying the defects to thermal equilibrium was postulated to be defect creation via electron-hole recombination, proportional to $np=n_i^2(T)$. If the $np$ product is reduced below equilibrium, the defect generation mechanism should be suppressed and the equilibrium defect density reduced. If these defects are of sufficient magnitude, they will affect the performance of *a*-Si:H–based devices. We now present evidence that the efficiency enhancement of *p-i-n* *a*-Si:H solar cells by the reverse-bias-anneal (RBA) treatment,[20] commonly interpreted as field-induced doping efficiency enhancement[7] of the *p* and *n* layers[8] is, in fact, a method to reduce the frozen-in defect density in the undoped *i* layer.

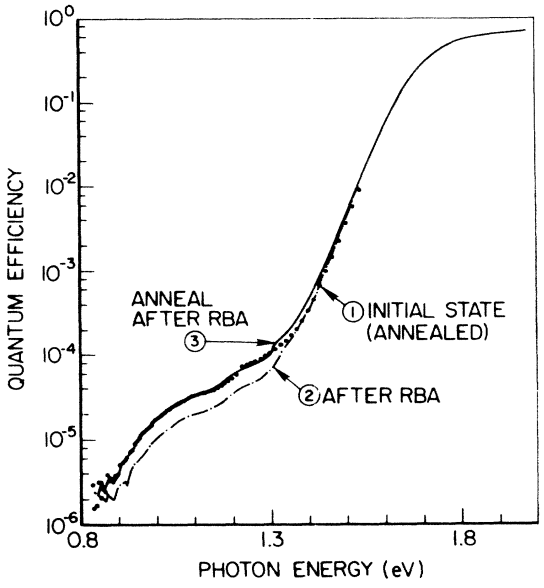


FIG. 3. Quantum efficiency (electrons per incident photon) of *a*-Si:H *p-i-n* solar cells. (1) Thermal anneal, no reverse bias; (2) annealed with reverse bias; (3) subsequent thermal anneal, no bias.

In the RBA technique, a solar cell structure is annealed at, typically, 200 °C for up to 1 h while a moderate reverse bias voltage is applied (5 V). As discussed in Ref. 4, the characteristics of the performance enhancement are just the reverse of the characteristics of light-induced performance degradation. As the latter appears controlled by the addition of dangling-bond defect states to the *i* layer,[21] this would imply that the RBA technique lowers the defect density in the *i* layer. Furthermore, the degree of performance enhancement as a function of anneal time[8] behaves as if the annealing activation energy were 1.4 eV, consistent with what one would expect for frozen-in defects in undoped *a*-Si:H (see Fig. 2).

For more direct experimental evidence, we measured the quantum efficiency[22] (number of electrons or holes collected per number of incident photons) for high efficiency ($\sim$10%) *p-i-n* solar cells[23] for photon energies at and below the band edge, before and after reverse-bias anneal. The results (Fig. 3) show that the RBA treat-

ment reduces subgap absorption. Furthermore, when the solar cell is subsequently annealed (again at 200 °C) without reverse bias, the initial state is restored. These results indicate that the defects in undoped *a*-Si:H are in thermal equilibrium at temperatures above 200 °C.

The difference between annealing with and without reverse bias is that the frozen-in defects are annealed out without being replaced by defects created by recombination of thermally generated electron-hole pairs. The reverse bias sweeps out carriers before they can recombine, lowering the *np* product below its equilibrium value $n_i^2(T)$. We can turn the argument around and surmise that the same mechanism produces the "field-enhanced doping" effect[7] in uniformly doped films.

We would like to thank R. Dawson and B. Shapo for experimental assistance. The program in amorphous semiconductors at Princeton University is supported by the Electric Power Research Institute under Contract No. RP2824-2. One of us (Z.E.S.) acknowledges receipt of an AT&T Bell Laboratories Scholarship.

*Note added.*—After submission of this manuscript, Müller *et al.* published calculations using chemical bonding considerations to predict equilibrium defect densities[24] independent of the kinetics of the mechanism driving the system towards equilibrium.

[1]D. L. Staebler and C. R. Wronski, Appl. Phys. Lett. **31**, 292 (1977).

[2]*Optical Effects in Amorphous Semiconductors—1984,* edited by P. C. Taylor and S. G. Bishop, AIP Conference Proceedings No. 120 (American Institute of Physics, New York, 1984).

[3]M. Stutzmann, W. B. Jackson, and C. C. Tsai, Phys. Rev. B **32**, 23 (1985).

[4]Z E. Smith and S. Wagner, Phys. Rev. B **32**, 5510 (1985).

[5]R. A. Street, J. Kakalios, and T. M. Hayes, Phys. Rev. B **34**, 3030 (1986).

[6]D. G. Ast and M. H. Brodsky, in *The Fourteenth International Conference on the Physics of Semiconductors,* edited by B. H. L. Wilson, Institute of Physics Conference Series No. 43 (Hilger, London, 1979), p. 1159.

[7]D. V. Lang, J. D. Cohen, and J. P. Harbison, Phys. Rev. Lett. **48**, 421 (1982).

[8]W. Krühler, H. Pfleiderer, R. Plättner, and W. Stetter, in *First International Photovoltaic Sciences and Engineering Conference,* edited by M. Konagai (Nippon, Tokyo, 1984), p. 127.

[9]D. Slobodin, S. Aljishi, R. Schwarz, and S. Wagner, in *Materials Issues in Applications of Amorphous Silicon Technology,* edited by D. Adler, A. Madan, and M. J. Thompson (Materials Research Society, Pittsburgh, 1985), p. 153.

[10]M. Vaněček, J. Kočka, J. Stuchlík, Z. Kožišek, O. Štika, and A. Tříska, Solar Energy Mater. **8**, 411 (1983).

[11]R. Schwarz, D. Slobodin, and S. Wagner, Appl. Phys. Lett. **47**, 740 (1985).

[12]T. Tiedje, in *Semiconductors and Semimetals Vol. 21C,* edited by J. Pankove (Academic, Orlando, 1984), p. 207.

[13]W. B. Jackson and N. Amer, Phys. Rev. B **25**, 5559 (1982).

[14]A. Skumanich, N. Amer, and W. B. Jackson, Phys. Rev. B **31**, 2263 (1985).

[15]Y. Bar-Yam, D. Adler, and J. D. Joannopoulos, Phys. Rev. Lett. **57**, 467 (1986).

[16]Z E. Smith, V. Chu, S. Aljishi, S. Wagner, and T. L. Chu, unpublished.

[17]Comparisons of ESR and PDS data (Ref. 13) find $N_s = C_0 \int \alpha dE$ with $C_0 = 7.9 \times 10^{15}$ cm$^{-2}$ eV$^{-1}$; our comparisons of ESR and CPM data find $C_0 \cong 1.9 \times 10^{16}$ cm$^{-2}$ eV$^{-1}$. The difference is due to the fact that CPM (being a photoconductive technique) sees only the transitions of an occupied deep state up to an extended conduction-band state.

[18]Z E. Smith and S. Wagner, J. Non-Cryst. Solids **77 & 78**, 1461 (1985).

[19]H. M. Branz, M. Meunier, S. Fan, J. H. Flint, J. S. Haggerty, and D. Adler, in *The Eighteenth IEEE Photovoltaic Specialists Conference* (IEEE, New York, 1986), p. 513.

[20]G. A. Swartz, Appl. Phys. Lett. **44**, 697 (1984).

[21]M. Hack and M. Shur, in Ref. 19, p. 1588; Z E. Smith, S. Wagner, and B. W. Faughnan, Appl. Phys. Lett. **46**, 1078 (1985).

[22]H. Kida, H. Yamagishi, T. Kamada, H. Okamoto, and Y. Hamakawa, in Ref. 8, p. 417.

[23]A. Catalano, R. V. D'Aiello, J. Dresner, B. Faughnan, A. Firester, J. Kane, H. Schade, Z E. Smith, G. Swartz, and A. Triano, in *The Sixteenth IEEE Photovoltaic Specialists Conference* (IEEE, New York, 1982), p. 1421.

[24]G. Müller, S. Kalbitzer, and H. Mannsperger, Appl. Phys. A **39**, 243 (1986).